PHYSICAL REVIEW B **77**, 020404(R) (2008)

Direct measurement of spin correlations using magnetostriction

V. S. Zapf,[1] V. F. Correa,[2,*] P. Sengupta,[1,3] C. D. Batista,[3] M. Tsukamoto,[4] N. Kawashima,[4] P. Egan,[1,5] C. Pantea,[1] A. Migliori,[1] J. B. Betts,[1] M. Jaime,[1] and A. Paduan-Filho[6]

[1]*National High Magnetic Field Laboratory (NHMFL), Los Alamos National Laboratory (LANL), Los Alamos, New Mexico 87545, USA*

[2]*NHMFL, Tallahassee, Florida 23210, USA*

[3]*T-11 Condensed Matter and Thermal Physics, LANL, Los Alamos, New Mexico 87545, USA*

[4]*Institute for Solid State Physics, University of Tokyo, Tokyo, Japan*

[5]*Oklahoma State University, Stillwater, Oklahoma 74078, USA*

[6]*Instituto de Fisica, Universidade de São Paulo, São Paulo, Brazil*

(Received 7 November 2007; published 9 January 2008)

We demonstrate that the short-range spin correlator $\langle \mathbf{S}_i \cdot \mathbf{S}_j \rangle$, a fundamental measure of the interaction between adjacent spins, can be directly measured in certain insulating magnets. We present magnetostriction data for the insulating organic compound $NiCl_2$-4SC$(NH_2)_2$, and show that the magnetostriction as a function of field is proportional to the dominant short-range spin correlator. Furthermore, the constant of proportionality between the magnetostriction and the spin correlator gives information about the spin-lattice interaction. Combining these results with the measured Young's modulus, we are able to extract dJ/dz, the dependence of the superexchange constant J on the Ni interionic distance z.

DOI: 10.1103/PhysRevB.77.020404 PACS number(s): 75.30.Et, 74.25.Ha, 75.10.Jm

INTRODUCTION

In magnetic systems, interactions between magnetic moments are responsible for the bulk of the phenomena that we seek to understand and exploit. The range, sign, geometrical configuration, and dependence on external parameters of the interactions play key roles in shaping the magnetic behavior of the system. In insulating magnets with transition metal ions, the dominant interactions are typically caused by superexchange between localized atomic magnetic moments that are comprised of electron spins. A key measure of these interactions is the short-range spin correlator between neighboring magnetic moments, $\langle \mathbf{S}_i \cdot \mathbf{S}_j \rangle$. This correlator is directly related to the magnetic energy and is one of the easiest quantities to compute theoretically. Very accurate values are often obtained even within approximate treatments. However, experimentally it is difficult to measure. Inelastic neutron scattering comes closest, but neutrons can measure the short-range spin correlator only for certain wave vectors q and frequencies ω. To determine $\langle \mathbf{S}_i \cdot \mathbf{S}_j \rangle$ we would have to measure and integrate over all q and ω, which is practically impossible. Thus, there is a wide gap between theory and experiment when it comes to short-range spin correlators. In this work, we show that magnetostriction measurements can be used to directly probe the short-range spin correlator and its dependence on interionic separation in quantum magnets with a single dominant exchange interaction. Since magnetostriction measurements can be performed to a very high degree of accuracy using capacitance techniques,[1] extremely accurate estimates of the short-range spin correlator can be obtained.

Additionally, we show that the same magnetostriction measurements can be used to estimate the strength of the spin-lattice coupling. Interplay of spin and lattice degrees of freedom can substantially change the strength of spin-spin interaction and in some cases induce instabilities such as the spin-Peierls transition. Knowledge of the short-range spin correlator and the strength of spin-lattice coupling are invaluable in developing a complete understanding of the various magnetic interactions in this class of magnetic insulators.

We test our approach by comparing magnetostriction measurements of $NiCl_2$-4SC$(NH_2)_2$ (DTN) to quantum Monte Carlo (QMC) computations of the nearest-neighbor spin correlator as a function of the applied magnetic field. An excellent agreement between the experimental and calculated curves combined with measurements of the elastic constant allows for an accurate determination of dJ/dz in DTN, where J is the strength of the superexchange interaction and z is the Ni interionic distance.

As already mentioned, this method is primarily applicable to magnets in which a single magnetic exchange J along one crystalline axis has the dominant dependence on lattice spacing, and the variation of other parameters with z can be neglected. This is fairly common in quantum magnets since superexchange results from overlap integral between adjacent molecular wave functions that have large radial dependencies with high power laws. This is in contrast to other on-site energy terms such as single-ion anisotropies that change more weakly as a function of the interion distance. For instance, previous experimental and theoretical works have modeled the spatial dependence of the superexchange interaction as a power law $J(z) \propto z^{-n}$ where z is the relevant spacing between magnetic ions. Values for the exponent n of 10–14 have been reported for metal halides,[2,3] and 2–7 for cuprates.[4,5]

RESULTS AND DISCUSSION

We now derive the relationship between the short-range spin correlator and the magnetostriction. The total energy density of a magnetic insulator can be written as the sum of the lattice and magnetic components, $\epsilon = \epsilon_e + \epsilon_m$, with

$$\epsilon_e = \frac{1}{2} E \left(\frac{z - z_0}{z_0} \right)^2, \quad \epsilon_m = \frac{1}{Nv} \langle \mathcal{H}_m \rangle, \tag{1}$$

where the magnetic Hamiltonian

$$\mathcal{H}_m = J(z)\sum_{\langle i,j\rangle} \mathbf{S}_i \cdot \mathbf{S}_j + \mathcal{H}'. \quad (2)$$

$\mathcal{H}'$ includes all the other magnetic interactions, which have a much weaker dependence on the interionic distance than the first term. Here $\langle i,j\rangle$ is a sum over nearest neighbors along the $\hat{\mathbf{z}}$ axis, and $z-z_0$ is the distortion of the interspin distance or bond length relative to its equilibrium value z_0 in the absence of magnetic interactions. E is the Young's modulus of the crystal along $\hat{z}$, v is the volume of the unit cell, and N is the total number of unit cells. We can now obtain the field dependence of z at $T=0$ by minimizing the total energy with respect to z and solving for the relative change in bond length

$$\frac{d\epsilon}{dz} = 0 \Rightarrow \frac{z-z_0}{z_0} = \frac{z_0}{vE}\frac{dJ}{dz}\langle \mathbf{S}_i \cdot \mathbf{S}_j\rangle. \quad (3)$$

Here we have used the Hellmann-Feynman theorem.[6,7] Since the magnetostriction is typically measured relative to $z(H=0)$ rather than z_0, it is convenient to rewrite Eq. (3) using $z(H=0)$ as the value of reference:

$$\frac{z(H)-z(0)}{z(0)} = \kappa(\langle \mathbf{S}_i \cdot \mathbf{S}_j\rangle_H - \langle \mathbf{S}_i \cdot \mathbf{S}_j\rangle_{H=0}), \quad (4)$$

where the proportionality constant is

$$\kappa = \frac{z_0}{vE}\frac{dJ}{dz}. \quad (5)$$

In principle, this analysis could be extended to three dimensions,[8,9] although calculations of the theoretical short-range spin correlator become more difficult perpendicular to the applied field direction. Similar calculations of the magnetostriction for hexagonal ferromagnetic systems have also been performed, although in this case the ferromagnetic order renders the spin-spin correlation function proportional to $\mathbf{S}^2$.[10] In conducting helical antiferromagnets, the relationship has been derived between the magnetostriction and the angle between spins in adjacent layers.[11]

Next we test our approach for the compound DTN. This material is an excellent test bed for the theory since the short-range spin correlator varies significantly and changes sign with magnetic field up to ~13 T, and the dominant exchange interactions are uniaxial and well studied, allowing us to compare theory with experiment.[12–15] DTN has previously attracted attention due to the possibility of Bose-Einstein condensation (BEC) occurring in the spin system.[14] A careful comparison between the theoretical Hamiltonian and experiment is of particular interest as possible symmetry changes induced by magnetostriction effects could affect the applicability of the BEC picture.

In DTN, the Ni atoms are arranged in a body-centered tetragonal structure as shown in Fig. 1. The strongest term in H_m is a single-ion anisotropy D that splits the Ni^{2+} $S=1$ levels into an $S^z=0$ ground state and $S^z=\pm 1$ excited levels. However, since D is an on-site interaction, its dependence on the interionic separation can be neglected. The dominant superexchange interaction $J_c=2.2$ K occurs along the Ni-Cl-Cl-Ni chains in the c axis; those along the a and b axes, $J_a=J_b=0.18$ K, are an order of magnitude smaller. No longer-range interactions have been found.[14,15]

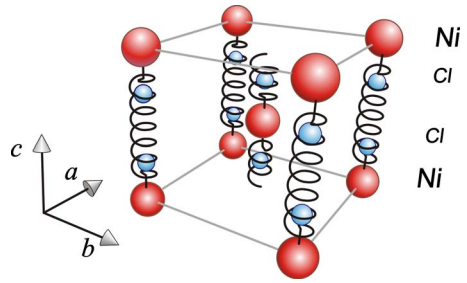

FIG. 1. (Color online) Unit cell of tetragonal $NiCl_2$-4SC$(NH_2)_2$ showing Ni (red, large) and Cl (blue, small) atoms. The thiourea molecules have been omitted for clarity.

The ground state of DTN is a quantum paramagnet at low fields due to the single-ion anisotropy D that forces the spins into the $S_z=0$ state. With an applied field parallel to the tetragonal c axis, the energy of the $S^z=-1$ is lowered due to the Zeeman effect until it becomes degenerate with the $S^z=0$ state at a critical field $H_{c1}=2.1$ T.[15] For $H>H_{c1}$, the mean value of each magnetic moment has a uniform z component along the field and a staggered xy component perpendicular to the field (canted antiferromagnet). With increasing field, this canted phase evolves continuously to a fully polarized spin state at $H_{c2}=12.6$ T. The evolution of the uniform component or magnetization as a function of field is shown in Fig. 2.

Magnetostriction measurements were performed on single crystals of DTN down to 25 mK in a 20 T magnet at the National High Magnetic Field Laboratory in Tallahassee, FL.[16] The magnetostriction as a function of H for $H\|c$ is shown in Fig. 3 for both the a and c axes of the crystal. The c-axis magnetostriction $\Delta L_c/L_c$ shows sharp shoulders at the boundaries of the ordered state at H_{c1} and H_{c2}, and nonmonotonic behavior in between. The a-axis lattice parameter decreases monotonically by an amount that is an order of magnitude smaller than the change in the c-axis parameter, reflecting the fact that $J_a \ll J_c$.

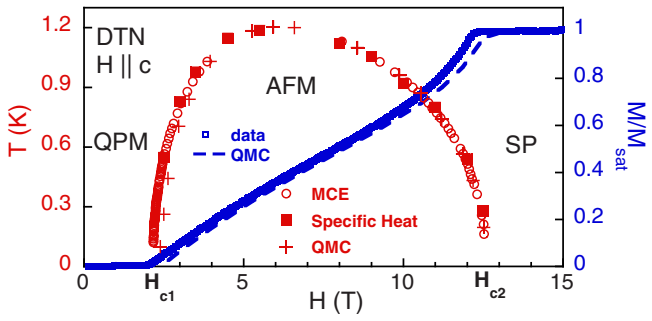

FIG. 2. (Color online) Temperature T vs magnetic field H phase diagram for $H\|c$ determined from specific heat and magnetocaloric effect (MCE) data, together with the result of quantum Monte Carlo simulations (Refs. 14 and 15). The magnetization vs field measured at 16 mK and calculated from QMC simulations is overlaid onto the phase diagram (Ref. 13). Regions of quantum paramagnetism (QPM), canted antiferromagnetism (AFM), and saturated paramagnetism (SP) are shown.

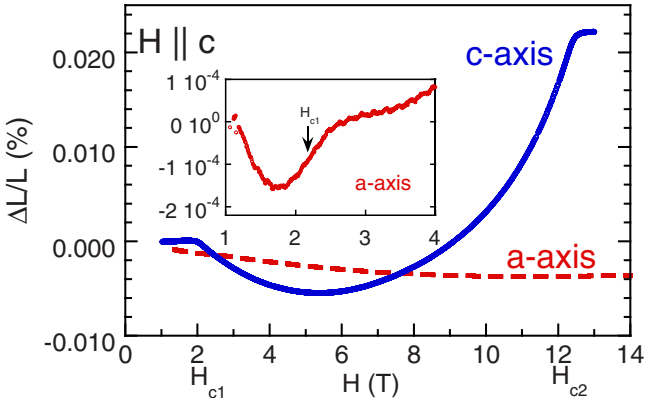

FIG. 3. (Color online) Normalized percentage length change $100\Delta L/L$ as a function of magnetic field measured along the crystallographic c axis (solid blue lines) and a axes (dashed red lines). The data are taken at $T=25$ mK with the magnetic field applied along the c axis. The inset shows the feature at H_{c1} in $100\Delta L_a/L_a$ in greater detail, and a straight line has been subtracted from the inset data for clarity (Ref. 16).

Here we focus on the c-axis magnetostriction, which according to our derivation should be proportional to the nearest-neighbor spin correlator along the tetragonal c axis. The field dependence between H_{c1} and H_{c2} is nonmonotonic due to a relative change of the antiferromagnetic and ferromagnetic spin components. For $H \gtrsim H_{c1}$, the uniform z component is smaller than the staggered xy component. As a result, the antiferromagnetic component is the dominant contribution to $\langle \mathbf{S}_i \cdot \mathbf{S}_j \rangle$ at low fields and creates an attractive magnetic force: by reducing the c-axis lattice parameter, the system increases J_c and lowers its magnetic energy. Since the canting angle (between the spin and the a-b plane) also increases with field, the ferromagnetic contribution eventually becomes dominant beyond $H \sim 5.5$ T. The ferromagnetic component increases the exchange energy of the bond and exerts an expansive force along the c axis to reduce J_c. Consequently, the nearest-neighbor spin correlator evolves from negative to positive between H_{c1} and H_{c2}.

We now compare the magnetostriction to the predicted nearest-neighbor spin correlator based on the Hamiltonian

$$\mathcal{H}_m = \sum_{\mathbf{r},\nu} J_\nu \mathbf{S}_\mathbf{r} \cdot \mathbf{S}_{\mathbf{r}+\mathbf{e}_\nu} + \sum_{\mathbf{r}} [D(S_\mathbf{r}^z)^2 - g\mu_B H S_\mathbf{r}^z], \qquad (6)$$

that has been determined by comparing magnetization, inelastic neutron scattering, and electron spin resonance measurements with spin-wave calculations and QMC simulations.[12–15] Here $\mathbf{e}_\nu = \{a\hat{\mathbf{x}}, b\hat{\mathbf{y}}, c\hat{\mathbf{z}}\}$ are the relative vectors between nearest-neighbor Ni ions, and g is the gyromagnetic ratio along the c axis.

Our QMC simulations were done on an $8\times8\times24$ lattice with the parameters $J_c=2.2$ K, $J_a=0.18$ K, and $D=8.6$ K.[15] We computed the correlator $\langle \mathbf{S}_\mathbf{r} \cdot \mathbf{S}_{\mathbf{r}+c\hat{\mathbf{z}}} \rangle$ as a function of field to obtain the magnetostriction curve via Eq. (4). The best agreement between the calculated curve and the measured magnetostriction (see Fig. 4) was obtained for

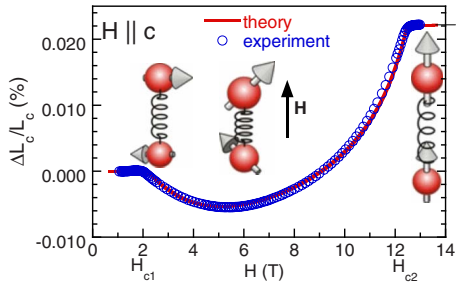

FIG. 4. (Color online) Comparison of experimental c-axis magnetostriction data as a function of H for $H \| c$ with the model described in the text.

$\kappa = 1.00\times10^{-5}$. The agreement is excellent, validating the model, and confirming our hypothesis that $|\partial D/\partial z| \ll |\partial J/\partial z|$.

Next we investigate the spin-lattice coupling in DTN. Since we already know κ, we can determine the spatial derivative of the antiferromagnetic exchange interaction dJ_c/dz from Eq. (5). The lattice parameters $a=b=9.558$ Å and $c=8.981$ Å are known from published x-ray diffraction measurements at 110 K,[17] leaving Young's modulus E as the remaining quantity to be measured in order to extract dJ_c/dz.

We have measured Young's modulus using resonant ultrasound spectroscopy between 300 and 5 K.[19,20] Mechanical resonances of a roughly cube-shaped single crystal of DTN were determined at zero field in a He-cooled Oxford Instruments flow cryostat and are shown in Fig. 5. The six independent elastic moduli were determined between 300 and 200 K, and their values at room temperature are shown in Fig. 5.

For lower temperatures, the determination of all of the resonances used in the fitting procedure became ambiguous. However, two good resonances were identified down to 5 K and, based on the temperature dependencies of these reso-

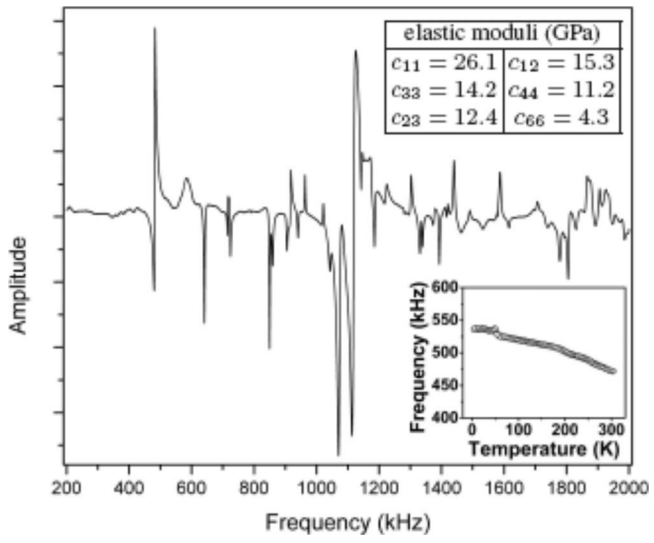

FIG. 5. Mechanical resonances of DTN at room temperature. Upper inset: Elastic moduli at room temperature. Lower inset: Temperature dependence of the major peak near 500 kHz between 5 and 300 K. The line is a fit to the Einstein oscillator model equation (Ref. 18) and used to extrapolate the resonance to 0 K.

nances, we extrapolated the value of Young's modulus to $T=0$ K. The value of the Young's modulus E along the c axis (E_{33}) in a tetragonal crystal is given by

$$E_{33} = C_{33} - \frac{2C_{13}^2}{C_{11} + C_{12}}, \tag{7}$$

yielding $E_{33}=7.5\pm0.7$ GPa at 0 K. By including this value in Eq. (5) we obtain $dJ_c/dz=2.5$ K/Å, yielding a total change in J_c between H_{c1} and H_{c2} of 5.5 mK or 0.25%. This in turn results in a 0.1% shift in H_{c2} relative to its value in the absence of magnetostriction effects. The dominant uncertainty in these calculations comes from the error bar in estimating Young's modulus due to the softness of the organic crystal. This introduces a systematic error in dJ/dz.

To our knowledge, the superexchange interaction and its spatial dependence in Ni-Cl-Cl-Ni chains has not been previously investigated experimentally or theoretically. For DTN, we speculate that the Cl-Cl bond determines the magnitude of dJ/dz along the Ni-Cl-Cl-Ni chains, since it is the weakest link, being nearly two times longer than the Ni-Cl bond (4.1 Å vs 2.4 or 2.5 Å). X-ray scattering studies have also implied[17] that the lowest-energy lattice vibrations consist of the $NiCl_2$-$4SC(NH_2)_2$ moving as a unit, thus supporting the idea that the Cl-Cl bonds that link adjacent molecules are more susceptible to pressure than the Ni-Cl bonds within a molecule. Although the relative variation of J between H_{c1} and H_{c2} is small (0.25%), recent electron spin resonance measurements demonstrate that the magnetic pressure may be inducing a structural instability that reduces the symmetry of the lattice.[21]

CONCLUSION

In summary, we discuss a method to measure the short-range spin correlator using magnetostriction measurements. We have applied this method to the compound $NiCl_2$-$4SC(NH_2)_2$ and we find that the measured magnetostriction curve is in excellent agreement with the one obtained from QMC simulations of $\mathcal{H}_m$. The same method allows us to obtain the degree of spin-lattice coupling. We expect this method to be widely applicable to other insulating magnets in which a uniaxial exchange interaction dominates the magnetostriction.

ACKNOWLEDGMENTS

This work was supported by the DOE, the NSF, and Florida State University through the National High Magnetic Field Laboratory. A.P.F. acknowledges support from CNPq (Conselho Nacional de Desenvolvimento Científico e Tecnológico, Brazil). We would like to thank S. Haas and N. Harrison for stimulating discussions.

*Present address: Comisión Nacional de Energía Atómica, Centro Atómico Bariloche, Argentina.

[1] G. M. Schmiedeshoff *et al.*, Rev. Sci. Instrum. **77**, 123907 (2006), and references therein.

[2] M. J. Massey, N. H. Chen, J. W. Allen, and R. Merlin, Phys. Rev. B **42**, 8776 (1990), and references therein.

[3] W. A. Harrison, *Electronic Structure and the Properties of Solids* (Freeman, San Francisco, 1980).

[4] M. C. Aronson, S. B. Dierker, B. S. Dennis, S.-W. Cheong, and Z. Fisk, Phys. Rev. B **44**, 4657 (1991).

[5] S. L. Cooper, G. A. Thomas, A. J. Millis, P. E. Sulewski, J. Orenstein, D. H. Rapkine, S.-W. Cheong, and P. L. Trevor, Phys. Rev. B **42**, 10785 (1990).

[6] H. Hellmann, *Quantenchemie* (Deuticke, Leipzig, 1937), p. 285.

[7] R. P. Feynman, Phys. Rev. **56**, 340 (1939).

[8] E. R. Callen, A. E. Clark, B. DeSavage, W. Coleman, and H. B. Callen, Phys. Rev. **130**, 1735 (1963).

[9] C. Kittel and J. H. V. Vleck, Phys. Rev. **118**, 1231 (1960).

[10] V. M. Kalita, I. M. Ivanova, and V. M. Loktev, Ukr. J. Phys. **50**, 1159 (2005).

[11] E. W. Lee, Proc. Phys. Soc. London **84**, 693 (1964).

[12] A. Paduan-Filho, R. D. Chirico, K. O. Joung, and R. L. Carlin, J. Chem. Phys. **74**, 4103 (1981).

[13] A. Paduan-Filho, X. Gratens, and N. F. Oliveira, Jr., Phys. Rev. B **69**, 020405(R) (2004).

[14] V. S. Zapf, D. Zocco, B. R. Hansen, M. Jaime, N. Harrison, C. D. Batista, M. Kenzelmann, C. Niedermayer, A. Lacerda, and A. Paduan-Filho, Phys. Rev. Lett. **96**, 077204 (2006).

[15] S. A. Zvyagin, J. Wosnitza, C. D. Batista, M. Tsukamoto, N. Kawashima, J. Krzystek, V. S. Zapf, M. Jaime, N. F. Oliveira, Jr., and A. Paduan-Filho, Phys. Rev. Lett. **98**, 047205 (2007).

[16] V. S. Zapf, V. F. Correa, C. D. Batista, T. P. Murphy, E. D. Palm, M. Jaime, S. Tozer, A. Lacerda, and A. Paduan-Filho, J. Appl. Phys. **101**, 09E106 (2007).

[17] A. Lopez-Castro and M. R. Truter, J. Chem. Soc. **1963**, 1309 (1963).

[18] Y. P. Varshni, Phys. Rev. B **2**, 3952 (1970).

[19] A. Migliori and J. Sarrao, *Resonant Ultrasound Spectroscopy* (Wiley, New York, 1997).

[20] A. Migliori, J. Sarrao, W. Visscher, T. Bell, M. Lei, Z. Fisk, and R. Leisure, Physica B **183**, 1 (1993).

[21] S. A. Zvyagin, A. K. Kolezhuk, V. N. Glazkov, S. S. Sosin, A. Smirnov, C. D. Batista, V. S. Zapf, M. Jaime, A. Paduan-Filho, and J. Wosnitza (unpublished).